



Evaluation of Dielectric Properties of Peanut Oil Biodiesel Mixed with Nano-additives

Pakalapati Janaki^{1*}, Surakasi Raviteja², Sista Deepthi³, Pappala Anil Kumar⁴,
Chandaka Durga Prasad¹ and Bhaskara Rao Amithi¹

¹Department of Electrical and Electronics Engineering, Lendi Institute of Engineering and Technology, Jonnada, Vizianagaram, AP, India

²Department of Mechanical Engineering, Lendi Institute of Engineering and Technology, Jonnada, Vizianagaram, AP, India

³Department of Basic Sciences and Humanities, Lendi Institute of Engineering and Technology, Jonnada, Vizianagaram, AP, India

⁴Department of Electrical and Electronics Engineering, Vignans Institute of Engineering for Women, Visakhapatnam, AP, India

Received: 06.02.2024 Accepted: 17.03.2024 Published: 30.03.2024

*Janaki.pakalapati@gmail.com



ABSTRACT

The main aim of this study is to assess the electrical characteristics pertaining to a biodiesel derived from peanut oil mixed with magnesium oxide (MgO) and zinc oxide (ZnO) nano-additives. After synthesizing biodiesel from peanut oil by the transesterification process, it is combined with MgO and ZnO nano-additives in varying proportions: 100 ppm MgO, 100 ppm ZnO and 50 ppm MgO + 50 ppm ZnO, of the overall volume. The measurement and analysis of biodiesel blends necessitate consideration of crucial electrical parameters, including breakdown voltage, resistivity, permittivity and electrical conductivity. A positive association was found between the quantity of nano-additives and resistivity. The potential cause for the enhancement of the electrical properties might be attributed to the dispersion of the nano-additives. The peanut oil dispersed with 100 ppm MgO exhibited desirable dielectric properties.

Keywords: Breakdown voltage; Permittivity; Resistivity; Electrical conductivity.

1. INTRODUCTION

Over the past few years, there seems to be a developing interest in peanut oil biodiesel as a renewable fuel option, which is increasingly being seen as a viable alternative to conventional fossil fuels. This shift in attention may be attributed to the environmental advantages associated with the use of peanut oil biodiesel (Franco *et al.* 2017; Cabaleiro *et al.* 2019; Kolcunová *et al.* 2017; García *et al.* 2020; Corach *et al.* 2017). However, biodiesel is subject to many restrictions such as insufficient cold flow properties, decreased oxidative stability and poor electrical conductivity (Julián *et al.* 2019; Corach *et al.* 2017). The possible influence of reduced electrical conductivity in biodiesel on fuel injection as well as ignition systems could lead to incomplete combustion resulting in a subsequent drop in engine performance (Aswin *et al.* 2022; Surakasi and Velivela, 2022; Julián *et al.* 2019). To mitigate this constraint, researchers have undertaken investigations on the use of lubricants as additives to enhance the electrical characteristics of biodiesel. The utilization of 20W-40T base lubricant as additives has been explored owing to its notable electrical conductivity and substantial surface area, as documented in previous studies. The impact of the base lubricant on the electrical characteristics of peanut oil biodiesel has been examined. This study intends to examine the electrical conductivity as well as dielectric strength associated with the fuel, both with and without the use of lubricating additives (Surakasi *et al.*

2023). The present work aims at conducting a comprehensive investigation on the influence of nanoparticle quantity and dimension on the electrical properties of the fuel.

2. PREPARATION OF BIODIESEL SAMPLES

Fig. 1 illustrates the biodiesel preparation process. The 1200 ml of peanut oil is subjected to a temperature of about 40 °C by a magnetic stirrer or mixer. The next step involves the amalgamation of 3.5 g of sodium hydroxide (KOH) pellets mixed with 125 ml of methanol. It is advisable to lower the temperature once the oil has reached a temperature range of 56 to 58 °C and then left as such for 1 h to undergo separation, facilitating the settling of the fatty acids and glycerol (Karthikeyan *et al.* 2020). Subsequently, a separating funnel was used as a means to separate the glycerol component from the oil. Following this, the oil was given a comprehensive washing with distilled water or heated water. The obtained oil was subjected to an extra warming procedure with a magnetic stirrer to elevate the temperature to 90 °C. The purpose of this step is to enhance the evaporation process of any water bubbles that could be present inside the oil. The collection and storage of oil should be carried out in specifically designed containers, which should be followed by an additional processing phase that involves the mixing of the oil (Raviteja *et al.* 2023). Fig. 2 shows a flow chart of various steps involved in the biodiesel preparation.

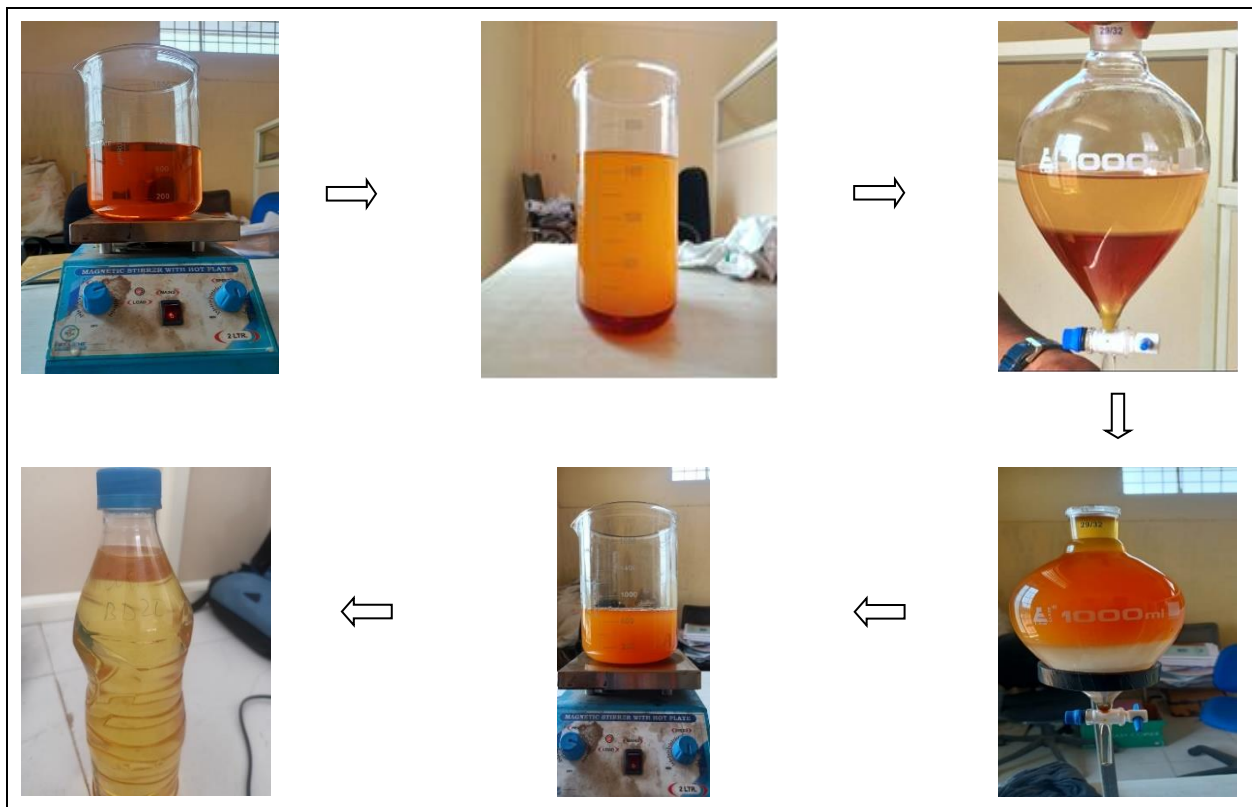


Fig. 1: Biodiesel preparation

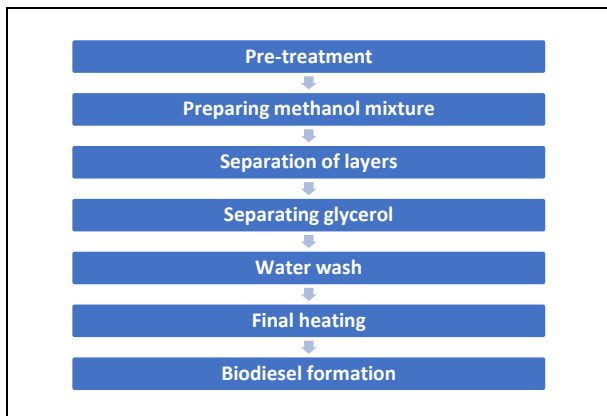


Fig. 2: Flow chart of Biodiesel preparation

2.1 Fuel Blending

The first step in the biodiesel blending process is the establishment of the desired blend ratio. In general, the proportion of biodiesel to diesel is often represented as a numerical percentage. After the appropriate blend ratio was established, the biodiesel was combined with MgO and ZnO nano-additives in varying proportions of 100 ppm MgO, 100 ppm ZnO and 50 ppm MgO + 50 ppm ZnO of the overall volume, using an Ultrasonicator equipment. The biodiesel blended with nano-additives

was used for analyzing breakdown voltage, dielectric constant, electrical conductivity and resistivity.

3. MATERIALS AND METHODOLOGY

3.1 Materials

| | |
|----------------|-----------------------------------------------------------------------|
| Oil sample | Peanut oil |
| Nano-additives | MgO and ZnO |
| Concentrations | 50 ppm and 100 ppm |
| Equipment | Laboratory stirrer, Magnetic stirrer, Transformer oil apparatus |

3.2 Breakdown Voltage

The term "breakdown voltage" is often used when referring to the minimum voltage necessary to induce electrical conduction inside a material. This indicates that there is a particular voltage at which the electrical resistance of the material reduces dramatically, making it possible for current to flow through it.

The occurrence of breakdown voltage might manifest in several ways, contingent upon the specific material and prevailing circumstances. Several prevalent forms of breakdown voltage include:

- ❖ Diodes with highly doped p-n junctions are prone to Zener breakdown. The Zener voltage is the reverse bias voltage above the junction, above which the junction opens to enable current to flow in the exact opposite direction.
- ❖ Avalanche breakdown is a phenomenon seen in some materials, particularly semiconductors when the application of a strong electric field results in the acquisition of sufficient kinetic energy by free electrons to dislodge more electrons. This initiates a cascading reaction, ultimately leading to the generation of a substantial electric current.
- ❖ When the electric field intensity exceeds a certain threshold, atoms and molecules within an insulating material become ionized, a process known as dielectric breakdown. This creates a channel for electrical current.

The determination of the breakdown voltage of a substance has significant importance in several electrical applications, and its value may be influenced by many variables including temperature, humidity and the existence of impurities or faults within the substance.

3.3 Dielectric Constant

The dielectric constant, which is also called the relative permittivity, is a way to measure how much electrical energy an object can store in an electric field. A material's internal electric flux density divided by its external electric flux density provides the relevant dimensionless number.

The dielectric constant measures how much an external electric field polarizes a material. Materials possessing a high dielectric constant can accumulate a substantial amount of electrical energy within an electric field; the materials characterized by a dielectric constant that is low exhibit a diminished ability to store such energy.

Electrical applications use the dielectric constant. In capacitor manufacture, it stores energy in an electric field. To store more energy, capacitors employ materials with a very high dielectric constant.

The dielectric constant is influenced by temperature, pressure and frequency. As a material's dielectric constant decreases with temperature, its electrical components may work poorly.

3.4 Electrical Conductivity

Electrical conductivity (denoted by the symbol σ), represents the quantitative assessment of a material's capacity to facilitate the flow of electrical current. A conductor refers to a substance that exhibits minimal resistance to the passage of electric current or heat energy. Materials can be categorized into three main groups: metals, semiconductors and insulators. The electrical conductivity of materials is a crucial characteristic in electronic applications. The utilization of mathematical models to estimate electrical conductivity presents an economically viable approach for assessing the electrical conductivity of materials composed of two or more constituents. There are various methodologies for the modeling of electrical conductivity in composites, which can be broadly classified into three main categories: simulation approaches, analytical-mathematical methods and image-processing methods. The units of conductivity are expressed as Siemens per meter (S/m), or more typically as milliSiemens per meter (mS/m). The Siemen, denoted as S, is the inverse of the Ohm (Ω), the standard unit of electrical resistance.

3.5 Resistivity

The word "resistivity" refers to the quality of a material that governs how well it blocks the flow of an electric current. Electrical conductivity, measured as the ratio of the applied electrical field to the resulting electrical current density, is a material's defining property.

Simply put, a substance's resistivity may be thought of as a numerical representation of how well or poorly it allows electric current to flow. Materials exhibiting high resistivity possess a pronounced level of electrical resistance and exhibit limited conductivity towards the electric current.

The resistivity of a material can be affected by various factors such as temperature and pressure, including the presence of impurities or defects within the material. As an example, it is observed that the resistivity of the majority of metals exhibits an upward trend as temperature rises, while semiconductors show a drop in resistance as temperature increases.

The attribute of resistivity has significant importance in several electrical applications, as it serves the purpose of assessing the electrical conductivity and efficiency of a given material. Understanding the resistance of a particular substance is also crucial when developing electric parts like cables as well as circuit boards.

4. EXPERIMENTAL SETUP



Fig. 4: Transformer oil apparatus

Parts:

1. Main switch
2. Fuse
3. Main pilot lamp L1
4. HT off push button
5. Motor control switch
6. HT on pilot lamp
7. Kilo voltmeter
8. L & N reserve pilot lamp
9. Earth open pilot lamp

4.1 Experimental Procedure

1. The procedure for this test involves the application of an ascending AC voltage, with a frequency range of 40-60 Hz, to the electrodes. The voltage was systematically incremented by 2 kV every second, commencing at zero and persisting until the voltage attained a threshold that induced breakdown. The transformer oil apparatus is shown in Fig. 4.
2. The experiment was conducted six times with the same cell filling.
3. The first voltage utilization should be promptly conducted after the cell has been filled, ensuring the absence of air bubbles and the presence of oil. This should be done within a maximum of 10 minutes after the filling process, after any previous breakdown.
4. The oil was carefully agitated inside the confines of the electrodes using sterile and desiccated glassware, to reduce the production of air bubbles. This process will condition the oil for later flue gas analysis. The voltage was re-established after a one-minute interval after the dissipation of any potential air bubbles. The absence of air bubbles was noted as a signal for the optimal time of voltage re-application.

5. RESULTS

5.1 Break Down Voltage

Fig. 5 illustrates the graph depicting the relationship between the distance and the corresponding breakdown voltage. It has been discovered that the voltage required for breakdown exhibited an increasing trend with the increase in distance. The maximum breakdown voltage was found to be 60 kV for the sample peanut oil - BD20 and the minimum breakdown voltage was found to be 48 kV for the sample BD20 + 100 ppm MgO. It can be concluded that varying the concentration of nano-additives tends to decrease the breakdown voltage.

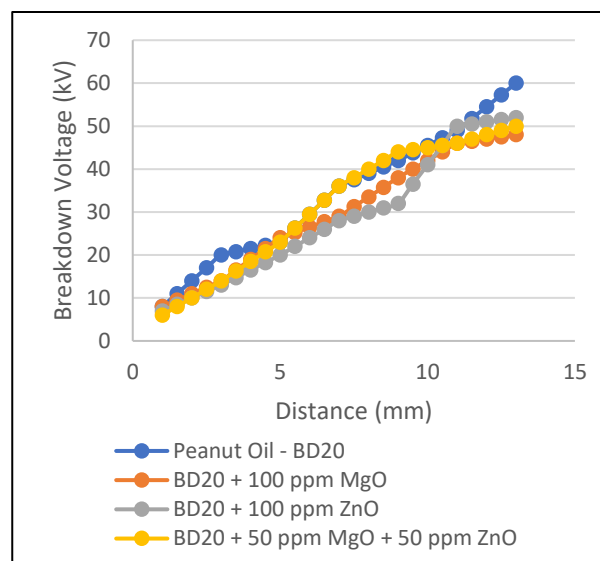


Fig. 5: Distance vs. Breakdown Voltage for Peanut oil - BD20

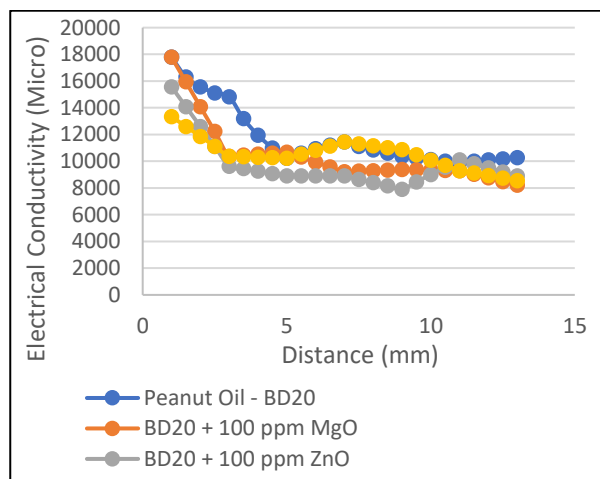


Fig. 6: Distance vs. Electrical conductivity for peanut oil - BD20

5.2 Electrical Conductivity

The plot of the Electrical Conductivity vs. distance is shown in Fig. 6. The values of electrical conductivity seem to follow a declining trend from 1 mm to 3 mm distance; later there is an increase in the value upto 5 mm distance. This trend again seems to decline upto 7.5 mm distance and then follows a linear trend upto the end. The maximum electrical conductivity was found to be 10265.17 for the sample peanut oil – BD20 and the was 8212.14 for the sample BD20 + 100 ppm MgO. It can be concluded that increasing the concentration of nano-additives tends to decrease the electrical conductivity.

5.3 Permittivity

The values of permittivity (Fig. 7) seem to follow a declining trend from 1 mm distance to 3 mm distance; later there is an increase in the value upto 5 mm distance. This trend again seems to decline upto 7.5 mm distance and then follows a linear trend upto the end. The maximum permittivity is found to be 4.615 for the sample peanut oil – BD20 and the minimum permittivity is found to be 3.692 for the sample BD20 + 100 ppm MgO. Thus, increasing the concentration of nano-additives tends to decrease the permittivity.

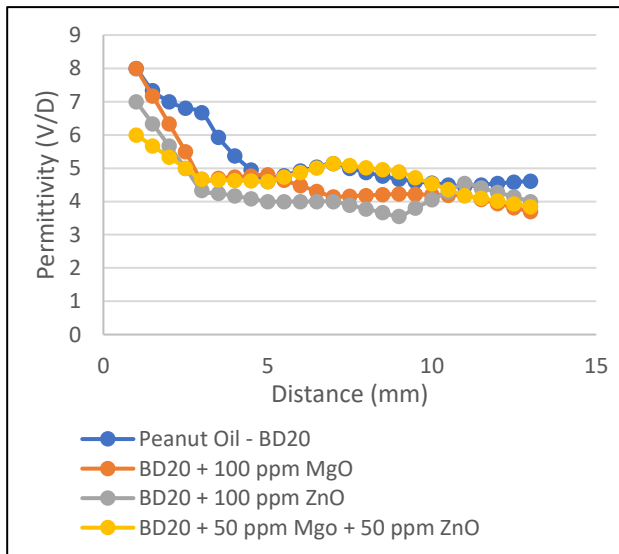


Fig. 7: Distance vs. Permittivity for peanut oil - BD20

5.4 Resistivity

The plot of the Resistivity vs. Distance is shown in Fig. 8. The values of resistivity seem to follow an increasing trend from 1 to 9 mm distance; later there is a decline in the value upto 11 mm distance and then increases till the end. The maximum resistivity was found to be 121.77 for the sample BD20 + 100 ppm MgO and the minimum resistivity was 97.42 for the sample peanut

oil - BD20. Thus, increasing the concentration of nano-additives tends to increase the resistivity.

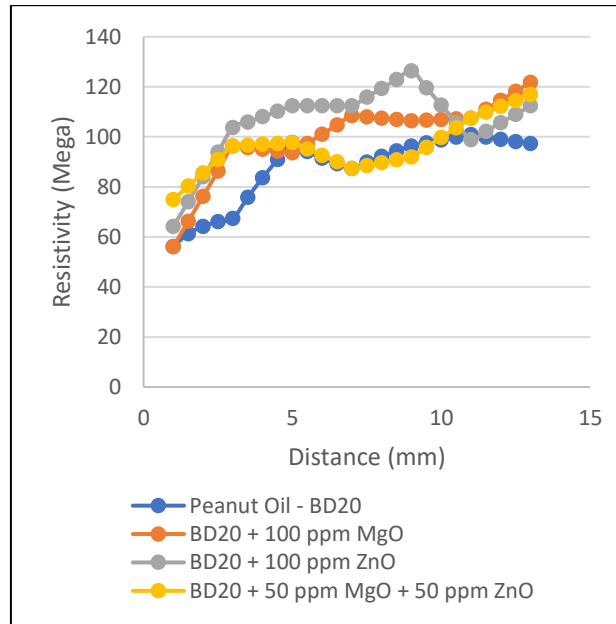


Fig. 8: Distance vs. Resistivity for peanut oil BD20

6. CONCLUSION

- ❖ The biodiesel is combined with MgO and ZnO nano-additives in varying proportions of 100 ppm MgO, 100 ppm ZnO and 50 ppm MgO + 50 ppm ZnO, of the overall volume, for improving engine performance and reducing emissions.
- ❖ The maximum breakdown voltage was found to be 60 kV for the sample peanut oil - BD20 and the minimum breakdown voltage was 48 kV for the sample BD20 + 100 ppm MgO. It can be concluded that varying the concentration of nano-additives tends to decrease the breakdown voltage.
- ❖ The maximum and minimum electrical conductivity were 10265.17 and 8212.14 for peanut oil - BD20 and BD20 + 100 ppm MgO, respectively. Thus, increasing the concentration of nano-additives tends to decrease the electrical conductivity.
- ❖ The trends for other parameters (permittivity and resistivity) were presented in a detailed manner in the previous section.
- ❖ Among the samples tested, peanut oil dispersed with 100 ppm MgO exhibited highly appreciable dielectric properties.
- ❖ Further research is needed to optimize the blending process and fully assess its potential benefits and drawbacks.

FUNDING

This research received no specific grant from any funding agency in the public, commercial, or not-for-profit sectors.

CONFLICTS OF INTEREST

The authors declare that there is no conflict of interest.

COPYRIGHT

This article is an open-access article distributed under the terms and conditions of the Creative Commons Attribution (CC BY) license (<http://creativecommons.org/licenses/by/4.0/>).



REFERENCES

- Aswin, C.G., Kumareswaran, A., Lakshmanan, R., Mathavan, S., Andal, V., Lakshmiathy, R. and Ivan, L. R. R., Comparative Analysis of NO_x Emission Reduction in Engines Using NiCo₂O₄ Nanoparticles without External Reductant at Low Temperatures: An Experimental Investigation, *J. Nanomater.*, 2022, 8981350 (2022). <https://doi.org/10.1155/2022/8981350>
- Cabaleiro, J. M., Paillat, T., Artana, G. and Touchard, G., Flow electrification in turbulent flows of liquids—comparison of two models for one specific case, *IEEE Trans. Ind. Appl.*, 55(5), 5235–5238 (2019). <https://dx.doi.org/10.1109/TIA.2019.2917053>
- Corach, J., Colman, M., Sorichetti, P. A. and Romano, S. D., Kinematic viscosity of soybean biodiesel and diesel fossil fuel blends: estimation from permittivity and temperature, *Fuel*, 207, 488-492 (2017). <https://doi.org/10.1016/j.fuel.2017.06.102>
- Corach, J., Sorichetti, P. A. and Romano, S. D., Permittivity of diesel fossil fuel and blends with biodiesel in the full range from 0% to 100%: application to biodiesel content estimation, *Fuel*, 188, 367-73 (2017). <https://doi.org/10.1016/j.fuel.2016.10.019>
- Franco, Jr. A., Pessoni, H. V. S. and Alves, T. E. P., Enhanced dielectric permittivity on yttrium doped cobalt ferrite nanoparticles, *Mater. Lett.*, 208, 115-117 (2017). <https://doi.org/10.1016/j.matlet.2017.04.101>
- García, M. M., Fernandez, S. S. D., Roman, C. and Delgado, M. A., Electro-active control of the viscous flow and tribological performance of ecolubricants based on phyllosilicate clay minerals and castor oil, *Appl. Clay Sci.*, 198, 105830 (2020). <https://doi.org/10.1016/j.clay.2020.105830>
- Julián, C., Eriel, F. G., Patricio, A. S. and Silvia, D. R., Broadband permittivity sensor for biodiesel and blends, *Fuel*, 254, 1-9 (2019). <https://doi.org/10.1016/j.fuel.2019.115679>
- Julián, C., Eriel, F. G., Patricio, A. S. and Silvia, D. R., Estimation of the composition of soybean biodiesel/soybean oil blends from permittivity measurements, *Fuel*, 235, 1309–1315 (2019). <https://doi.org/10.1016/j.fuel.2018.08.114>
- Karthikeyan, S., Prathima, A., Periyasamy, M. and Mahendran, G., Performance analysis of Al₂O₃ and C₁₈H₃₄O₂ with Kappaphycus Alvarezil-Brown algae biodiesel in CI engine, *Elsev. Mater. Today Proceed.*, 33, 4180-4184 (2020). <https://doi.org/10.1016/j.matpr.2020.07.118>
- Kolcunová, I., Kurimský, J., Cimbala, R., Petráš, J., Dolník, B., Džmura, J. and Balogh, J., Contribution to static electrification of mineral oils and natural esters, *J. Electrostat.*, 88, 60-64 (2017). <http://dx.doi.org/10.1016/j.elstat.2017.01.024>
- Raviteja, S., Janaki, P., Ramya, P. and Trinadh, B. K., Characterization and Evaluation of Electrical Properties of corn Oil Biodiesel mixed with Nano Additive, *Int. J. Renewable Energy Res.*, 13(2), 1-7 (2023). <https://doi.org/10.20508/ijrer.v13i2.14144.g8742>
- Surakasi, R. and Velivela, L. C., Liquid Fuels Derived from Microalgae: Physicochemical Analysis, *J. Eng.*, 2022, 1-5 (2022). <https://doi.org/10.1155/2022/1293310>
- Surakasi, R., Srinivasa, R. Y., Kalam, S. A. and Begum, N., Emissions and Performance of Diesel Engines Correlated with Biodiesel Properties, *J. Eng.*, 2023, 1-4 (2023). <https://doi.org/10.1155/2023/5274325>